Iranian Journal of Mathematical Sciences and Informatics
Vol. 4, No. 1 (2009), pp. 55-77
DOI: 10.7508/ijmsi.2009.01.006

Axisymmetric Vibrations in Micropolar Thermoelastic Cubic Crystal Plate Bordered with Layers or Half Spaces of Inviscid liquid

Rajneesh Kumar[a] and Geeta Partap[b,*]

[a]Department of Mathematics, Kurukshetra University, Kurukshetra, Haryana, India - 136 119
[b]Department of Mathematics, Dr. B. R. Ambedkar National Institute of Technology, Jalandhar, Punjab, India -144 011

E-mail: rajneesh_kuk @ rediffmail.com
E-mail: pratapg@nitj.ac.in, gp.recjal@gmail.com

Abstract. The present study is concerned with the propagation of axisymmetric vibrations in a homogenous isotropic micropolar thermoelastic cubic crystal plate bordered with layers or half spaces of inviscid liquid subjected to stress free boundary conditions in context of Lord and Shulman (L-S) and Green and Lindsay (G-L) theories of thermoelasticity. The secular equations for symmetric and skew-symmetric leaky and nonleaky Lamb wave modes of propagation are derived. The amplitudes of displacement components, microrotation and temperature distribution are also computed numerically and presented graphically. Finally, in order to illustrate the analytical developments, numerical solution of secular equations corresponding to stress free thermally insulated micropolar thermoelastic cubic crystal plate is carried out for magnesium crystal material bordered with water layers of finite and infinite thickness.

Keywords: Micropolar thermoelastic cubic crystal plate; secular equations; Phase velocity; Symmetric and skew-symmetric amplitudes; Attenuation coefficient.

2000 Mathematics subject classification: 74A, 74B, 74F, 74J, 74K.

*Corresponding Author

Accepted 15 September 2009

1. Introduction

The problem of wave propagation in an elastic plate of uniform material was first investigated by Lamb [1]. Since then the term Lamb wave has been used to refer to an elastic disturbance propagating in a solid plate with free boundaries. Lamb waves have found applications in multi-sensors and in the inspection of defects in thin – walled materials. The density and viscosity sensing with Lamb waves is based on the principle that the presence of liquid in contact with a solid plate changes the velocity and amplitude of the Lamb waves in the plate with free boundaries. When a plate of finite thickness is bordered with homogeneous liquid half spaces on both sides, then some part of the Lamb wave energy in the plate radiates into the liquid, while most of the energy still remains in the solid. These are known as leaky Lamb waves. Wu and Zhu [2] and Zhu and Wu [3] studied the propagation of Lamb waves in an elastic plate when both sides of the plate are bordered with liquid layers.

Nayfeh and Nagy [4] derived the exact characteristic equations for leaky waves propagating along the interfaces of several systems involving isotropic elastic solids loaded with viscous fluids, including semi-spaces and finite thickness plates totally immersed in fluids or coated on one or on both sides by finite thickness fluid layers. The technique adopted by Nayfeh and Nagy [4] removed certain inconsistencies that unnecessarily reduce the accuracy and range of validity of the Zhu and Wu [3] results.

The classical theory of elasticity is inadequate to represent the behavior of some modern engineering structures such as polycrystalline materials and materials with fibrous or coarse grain. The study of these materials requires incorporation of theory of oriented media. "Micropolar elasticity", termed by Eringen [5], is used to describe the deformation of elastic media with oriented particles. A micropolar continuum is a collection of interconnected particles in the form of small rigid bodies undergoing both translational and rotational motions. The force at a point of a surface element of bodies of these materials is completely characterized by a stress vector and a couple stress vector at that point.

The linear theory of micropolar thermoelasticity was developed by extending the theory of micropolar continua to include thermal effects by Eringen [6] and Nowacki [7]

Following various methods, the elastic fields of various loadings, inclusion and inhomogeneity problems, and interaction energy of point defects and dislocation arrangement have been discussed extensively in the past. Generally all materials have elastic anisotropic properties which mean the mechanical behavior of an engineering material characterized by the direction dependence. However the three-dimensional study for an anisotropic material is much more

complicated to obtain than the isotropic one, due to the large number of elastic constants involved in the calculation.

A wide class of crystals such as W, Si, Cu, Ni, Fe, Au, Al, etc., which are some frequently used substances, belong to cubic materials. The cubic materials have nine planes of symmetry whose normals are on the three coordinate axes and on the coordinate planes making an angle $\pi/4$ with the coordinate axes. With the chosen coordinate system along the crystalline directions, the mechanical behavior of a cubic crystal can be characterized by four independent elastic constants A_1, A_2, A_3 and A_4.

To understand the crystal elasticity of a cubic material, Chung and Buessem [8] presented a convenient method to describe the degree of the elasticity anisotropy in a given cubic crystal. Later, Lie and Koehler [9] used a Fourier expansion scheme to calculate the stress fields caused by a unit force in a cubic crystal. Minagawa et al. [10] discussed the propagation of plane harmonic waves in a cubic micropolar medium. Kumar and Rani [11] studied time harmonic sources in a thermally conducting cubic crystal. However no attempt has been made to study source problems in micropolar cubic crystals. Kumar and Ailawalia [12] investigated elastodynamics of inclined loads in micropolar cubic crystals. Kumar and Ailawalia [13] studied time harmonic sources at micropolar thermoelastic medium possessing cubic crystals with one relaxation time. Kumar and Singh [14] investigated propagation of plane waves in thermoelastic cubic crystal material with two relaxation times. Kumar and Kansal [15] discussed the analysis of wave motion in transversely isotropic generalized thermoelastic diffusive plate. Sharma and Kumar [16] examined Lamb waves in micropolar thermoelastic solid plates immersed in liquid with varying temperature.

In practical situations, it is extremely important to hidden cracks and other possible faults in aerospace and other structures. This can be done by using ultrasonic waves. Lamb waves which direct the energy along the plate are especially useful in thin plates. The other applications are in radar detection. Recently, resurgent interest in Lamb waves is initiated by its applications in multisensors.

The present investigation is concerned to study the propagation of axisymmetric vibrations in an infinite homogeneous isotropic micropolar thermoelastic plate possessing cubic symmetry bordered with layers or half space of inviscid liquid.

2. Formulation of the problem

We consider an infinite homogeneous isotropic, thermally conducting micropolar thermoelastic cubic crystal plate of thickness 2d and initially at uniform temperature T_0. The plate is bordered with infinitely large homogeneous inviscid liquid half spaces or layers of thickness h on both sides. The plate is

axi-symmetric with respect to z – axis as the axis of symmetry. We take origin of the co-ordinate system (r,θ, z) on the middle surface of the plate and the z – axis is taken normal to the solid plate along the thickness. We take r – z plane as the plane of incidence.

If we restrict our analysis to plane strain problem parallel to r–z plane with displacement vector $\vec{u} = (u_r, 0, u_z)$and microrotation vector $\vec{\phi} = (0, \phi_\theta, 0)$, then the field equations and constitutive relations in a micropolar thermoelastic solid with cubic symmetry in the absence of body forces, body couples and heat sources are given by Minagawa et al [10], Lord and Shulman [17] and Green and Lindsay [18]

$$A_1(\frac{\partial^2 u_r}{\partial r^2} + \frac{1}{r}\frac{\partial u_r}{\partial r} - \frac{u_r}{r^2}) + A_3\frac{\partial^2 u_r}{\partial z^2} + (A_2 + A_4)\frac{\partial^2 u_z}{\partial r \partial z} - (\mathrm{A}_3 - A_4)\frac{\partial \phi_\theta}{\partial z} - \nu\frac{\partial}{\partial r}(1 + \tau_1\frac{\partial}{\partial t})T = \rho\frac{\partial^2 u_r}{\partial t^2}, \tag{1}$$

$$A_1\frac{\partial^2 u_z}{\partial z^2} + A_3(\frac{\partial^2 u_z}{\partial r^2} + \frac{1}{r}\frac{\partial u_z}{\partial r}) + (A_2 + A_4)(\frac{\partial^2 u_r}{\partial r \partial z} + \frac{1}{r}\frac{\partial u_r}{\partial z}) + (\mathrm{A}_3 - A_4)(\frac{\partial \phi_\theta}{\partial r} + \frac{\phi_\theta}{r}) - \nu\frac{\partial}{\partial z}(1 + \tau_1\frac{\partial}{\partial t})T = \rho\frac{\partial^2 u_z}{\partial t^2}, \tag{2}$$

$$B_3(\frac{\partial^2 \phi_\theta}{\partial r^2} + \frac{\partial^2 \phi_\theta}{\partial z^2} + \frac{1}{r}\frac{\partial \phi_\theta}{\partial r} - \frac{\phi_\theta}{r^2}) + (A_3 - A_4)(\frac{\partial u_r}{\partial z} - \frac{\partial u_z}{\partial r} - 2\phi_\theta) = \rho\, j\frac{\partial^2 \phi_\theta}{\partial t^2}, \tag{3}$$

$$K^*(\frac{\partial^2}{\partial r^2} + \frac{1}{r}\frac{\partial}{\partial r} + \frac{\partial^2}{\partial z^2})T = \rho\, C^*(\frac{\partial T}{\partial t} + \tau_0\frac{\partial^2 T}{\partial t^2}) + \nu T_0(\frac{\partial}{\partial t} + \eta_0\tau_0\frac{\partial^2}{\partial t^2})(\frac{\partial u_r}{\partial r} + \frac{\partial u_z}{\partial z} + \frac{u_r}{r}), \tag{4}$$

$$t_{zz} = A_1\frac{\partial u_z}{\partial z} + A_2(\frac{\partial u_r}{\partial r} + \frac{u_r}{r}) - \nu(1 + \tau_1\frac{\partial}{\partial t})T, \tag{5}$$

$$t_{zr} = A_3\frac{\partial u_r}{\partial z} + A_4\frac{\partial u_z}{\partial r} + (A_4 - A_3)\phi_\theta, \tag{6}$$

$$m_{z\theta} = B_3\frac{\partial \phi_\theta}{\partial z}. \tag{7}$$

where $A = A_1 - A_2 - A_3 - A_4$, $B = B_1 - B_2 - B_3 - B_4$, $\nu = (A_1 + 2A_2)\alpha_t$. A_1, A_2, A_3, A_4, B_1, B_2, B_3, B_4 are material constants, α_t is coefficient of linear thermal expansion, ρ is the density, j is the microinertia, t_{ij} and m_{ij} are the components of stress and couple stress tensors respectively,$K^*$is the coefficient of thermal conductivity, C^* is specific heat at constant strain,τ_0 and τ_1 are thermal relaxation times ,δ_{ij} is Kronecker delta. The comma notation denotes spatial derivatives.

For Lord and Shulman(L – S) theory $\tau_1 = 0$, $\tau_0 > 0$ and $\eta_0 = 1$ and for Green and Lindsay (G – L) theory $\tau_1 \geq \tau_0 > 0$ and $\eta_0 = 0$.

For the liquid half – space, the equation of motion and constitutive relations are given by

$$\lambda_L\nabla(\nabla.\vec{u}_L) = \rho_L\frac{\partial^2 \vec{u}_L}{\partial t^2}, \tag{8}$$

$$(t_{ij})_L = \lambda_L (u_{r,r})_L \delta_{ij}. \tag{9}$$

We define the non-dimensional quantities

$r' = \frac{\omega^* r}{c_1}, z' = \frac{\omega^* z}{c_1}, u'_r = \frac{\rho\omega^* c_1}{\nu T_0} u_r, u'_z = \frac{\rho\omega^* c_1}{\nu T_0} u_z, t' = \omega^* t, \phi'_\theta = \frac{\rho c_1^2}{\nu T_0}\phi_\theta,$
$T' = \frac{T}{T_0}, t'_{ij} = \frac{1}{\nu T_0} t_{ij},$

$$\tau'_0 = \omega^* \tau_0, \tau'_1 = \omega^* \tau_1, m'_{ij} = \frac{\omega^* m_{ij}}{c_1 \nu T_0}, H' = \frac{c_1 H}{\omega^*}, \tag{10}$$

$$c_L^2 = \frac{\lambda_L}{\rho_L}, u'_L = \frac{\rho_L \omega^* c_1}{\nu T_0} u_L, w'_L = \frac{\rho_L \omega^* c_1}{\nu T_0} w_L \ .$$

where $c_1^2 = \frac{A_1}{\rho}$, $\omega^* = \frac{\rho\, C^* c_1^2}{K^*}$, ω^* is the characteristic frequency of the medium, c_L is the velocity of sound in the liquid, ρ_L is the density of the liquid and λ_L is the bulk modulus.

Using equation (10) in equations (1) - (4) and (8) and after suppressing the primes for convenience, we obtain

$$d_1\left(\frac{\partial^2 u_r}{\partial r^2} + \frac{1}{r}\frac{\partial u_r}{\partial r} - \frac{u_r}{r^2}\right) + d_2 \frac{\partial^2 u_r}{\partial z^2} + d_3 \frac{\partial^2 u_z}{\partial r \partial z} - \tag{11}$$

$d_4 \frac{\partial \phi_\theta}{\partial z} - \frac{\partial}{\partial r}(1 + \tau_1 \frac{\partial}{\partial t})T = \frac{\partial^2 u_r}{\partial t^2},$

$$d_1 \frac{\partial^2 u_z}{\partial z^2} + d_2\left(\frac{\partial^2 u_z}{\partial r^2} + \frac{1}{r}\frac{\partial u_z}{\partial r}\right) + d_3\left(\frac{\partial^2 u_r}{\partial r \partial z} + \frac{1}{r}\frac{\partial u_r}{\partial z}\right) + \tag{12}$$

$d_4\left(\frac{\partial \phi_\theta}{\partial r} + \frac{\phi_\theta}{r}\right) - \frac{\partial}{\partial z}(1 + \tau_1 \frac{\partial}{\partial t})T = \frac{\partial^2 u_z}{\partial t^2},$

$$\left(\frac{\partial^2 \phi_\theta}{\partial r^2} + \frac{\partial^2 \phi_\theta}{\partial z^2} + \frac{1}{r}\frac{\partial \phi_\theta}{\partial r} - \frac{\phi_\theta}{r^2}\right) - \tag{13}$$

$d_5\left(\frac{\partial u_r}{\partial z} - \frac{\partial u_z}{\partial r}\right) - 2d_5\phi_\theta = d_6 \frac{\partial^2 \phi_\theta}{\partial t^2},$

$$\nabla^2 T = \left(\frac{\partial T}{\partial t} + \tau_0 \frac{\partial^2 T}{\partial t^2}\right) + \in \left(\frac{\partial}{\partial t} + \eta_0 \tau_0 \frac{\partial^2}{\partial t^2}\right)\left(\frac{\partial u_r}{\partial r} + \frac{\partial u_z}{\partial z} + \frac{u_r}{r}\right), \tag{14}$$

$$\delta_L^2\left(\frac{\partial^2 u_{L_i}}{\partial r^2} + \frac{1}{r}\frac{\partial u_{L_i}}{\partial r} - \frac{u_{L_I}}{r^2} + \frac{\partial^2 w_{L_i}}{\partial r \partial z}\right) = \frac{\partial^2 u_{L_i}}{\partial t^2}, \tag{15}$$

$$\delta_L^2\left(\frac{\partial^2 u_{L_i}}{\partial r \partial z} + \frac{1}{r}\frac{\partial w_{L_i}}{\partial z} + \frac{\partial^2 w_{L_i}}{\partial z^2}\right) = \frac{\partial^2 w_{L_i}}{\partial t^2}. \tag{16}$$

where $d_1 = \frac{A_1}{\rho\, c_1^2}$, $d_2 = \frac{A_3}{\rho\, c_1^2}$, $d_3 = \frac{A_2+A_4}{\rho\, c_1^2}$, $d_4 = \frac{A_3-A_4}{\rho\, c_1^2}$, $d_5 = \frac{(A_3-A_4)\, c_1^2}{B_3\omega^*}$, $d_6 = \frac{\rho\, j\, c_1^2}{B_3}$,

$$\in= \frac{\nu^2 T_0}{\rho\omega^* K^*}, \delta_L^2 = \frac{c_L^2}{c_1^2}, \nabla^2 = \frac{\partial^2}{\partial r^2} + \frac{1}{r}\frac{\partial}{\partial r} + \frac{\partial^2}{\partial z^2}.$$

In the liquid boundary layers, we have

$$u_{L_i} = \frac{\partial \phi_{L_i}}{\partial r} + \frac{\partial \psi_{L_i}}{\partial z} \tag{17}$$

and

$w_{L_i} = \frac{\partial \phi_{L_i}}{\partial z} - \frac{\partial \psi_{L_i}}{\partial r} - \frac{\psi_{L_i}}{r}$

where ϕ_{L_i} and ψ_{L_i} are the respectively the scalar velocity potential and vector velocity component along the θ – direction, for the top liquid layer (i = 1) and for the bottom liquid layer (i = 2), $u_{L_i}$and $w_{L_i}$are respectively , the r and z components of particle velocity.

Using equations (17) in equations (15) and (16), we obtain

$$\nabla^2 \phi_{L_i} - \frac{1}{\delta_L^2}\frac{\partial^2 \phi_{L_i}}{\partial t^2} = 0; i = 1, 2. \tag{18}$$

Because the inviscid liquid does not support the shear motion so shear modulus of liquid vanishes and hence ψ_{L_i}, i = 1,2 vanish. The potential function ϕ_{L_i}in case of inviscid liquid layers satisfy the equation (18).

3. Formal solution of the problem

We assume the solution of equations (11) – (14) and (18) of the type

$$(u_r, u_z, \phi_\theta, T, \phi_{L_1}, \phi_{L_2}) = \tag{19}$$

$$\left[J_1(\xi r), \bar{u}_z J_0(\xi r), \bar{\phi}_\theta J_1(\xi r), \bar{T} J_0(\xi r), \bar{\phi}_{L_1} J_0(\xi r), \bar{\phi}_{L_2} J_0(\xi r)\right]\ \bar{u}_r\ e^{i\xi(mz-ct)}.$$

where $c = \frac{\omega}{\xi}$ is the phase velocity of the wave ,ω is the angular frequency and ξ is the wave number.

m is an unknown parameter which signifies the penetration depth of the wave; $\bar{u}_z, \bar{\phi}_\theta, \bar{T}$ are the amplitude ratios of displacement u$-z$, microrotation ϕ_θ and temperature T to that of displacement u$-r$ respectively.

Using equation (19) in equations (11) – (14), we obtain

$$\frac{m^2}{c^2} + a_1 + m a_2 \bar{u}_z + m a_3 \bar{\phi}_\theta + a_4 \bar{T} = 0, \tag{20}$$

$$ma_5 + \frac{(m^2 + a_6)}{c^2}\bar{u}_z + a_7\bar{\phi}_\theta + ma_8\bar{T} = 0, \tag{21}$$

$$ma_9 - a_9\bar{u}_z - (\frac{m^2+1}{c^2} + a_{10} + a_{13})\bar{\phi}_\theta = 0, \tag{22}$$

$$a_{11} + ma_{11}\bar{u}_z - \frac{m^2}{c^2}\bar{T} + a_{12}\bar{T} = 0. \tag{23}$$

The system of equations (20) – (23) has a non-trivial solution if the determinant of coefficients of $(1, \bar{u}_z, \bar{\phi}_\theta, \bar{T})^T$ vanishes,which yields an algebraic equation relating m to c.
Solving the above equations, we obtain an eight degree equation of the form

$$m^8 + A'm^6 + B'm^4 + C'm^2 + D' = 0. \tag{24}$$

The roots of the equation (24) give four values of m^2.
Using a computer program of Descard's method following Cardan's method, equation (24) leads to the following solution for displacements, microrotation and temperature as

$$(u_r, u_z, \phi_\theta, T) = \tag{25}$$

$\sum_{i=1}^{4}[E_i Cos\ \xi m_i z + F_i Sin\ \xi m_i z]\{J_1(\xi r), r_i J_0(\xi r), l_i J_1(\xi r), t_i J_0(\xi r)\}e^{-i\omega t}$.

Again using solution (19) in equation (18), we obtain

$$\phi_{L_1} = (E_5 e^{\gamma_L z} + F_5 e^{-\gamma_L z})J_0(\xi r)e^{-i\omega t}, \tag{26}$$

$$\phi_{L_2} = (E_6 e^{\gamma_L z} + F_6 e^{-\gamma_L z})J_0(\xi r)e^{-i\omega t}. \tag{27}$$

where $\gamma_L^2 = \xi^2(1 - \frac{c^2}{\delta_L^2})$,$A' = A^*c^2 + 4$,$B' = B^*c^4 + 3A^*c^2 + 6$, $C' = G^*c^6 + 2B^*c^4 + 3A^*c^2 + 4$,$D' = D^*c^8 + G^*c^6 + B^*c^4 + A^*c^2 + 1$,

$$A^* = [(a_{16} - a_{20} - k_0 + a_{21}) + c^2(a_8a_{20} - a_2a_5 + a_3a_9)],$$

$$B^* = [(k_0a_{20} - k_0a_{16} - a_{16}a_{20} - a_7a_9 - a_8a_{20} + a_2a_5 + a_{21}a_{16} - a_{21}a_{20} - k_0a_{21} - a_3a_9 + a_4a_{11}) + c^2(k_0a_2a_5 - a_8a_{20}a_{11} + a_2a_5a_{20} - a_2a_7a_9 + a_2a_8a_{11} + a_{21}a_{20}a_8 + a_3a_5a_9 - k_0a_3a_9 - a_3a_{16}a_9 - a_4a_5a_{11} + c^2a_3a_8a_9a_{11})]$$

$$G^* = [(a_8a_{20}a_{11} + k_0a_{16}a_{20} + k_0a_7a_9 - k_0a_2a_5 - a_2a_5a_{20} + a_2a_7a_9 - a_2a_8a_{11} - a_3a_5a_9 + k_0a_3a_9 + a_3a_6a_9 - a_4a_{20}a_{11} + a_4a_5a_{11} + a_4a_6a_{11}) + a_{21}(k_0a_{20} - k_0a_6 - a_{16}a_{20} - a_7a_9 - a_8a_{20}) + c^2(k_0a_2a_7a_9 - k_0a_2a_5a_{20} - a_2a_8a_{20}a_{11} - a_{21}a_8a_{20}a_{11} + k_0a_3a_5a_9 + k_0a_3a_{16}a_9 - a_3a_8a_9a_{20} - a_4a_7a_9a_{11} + a_4^2a_5a_{20})]$$

$$D^* = k_0a_2a_5a_{20} - k_0a_2a_7a_9 + a_2a_8a_{20}a_{11} + a_{21}a_8a_{20}a_{11} + k_0a_{21}a_{16}a_{20} + k_0a_{21}a_7a_9 + k_0a_3a_5a_9 + k_0a_3a_{16}a_9 + a_4a_5a_{20}a_{11} + a_4a_{16}a_{20}a_{11}$$

$$a_1 = \frac{(d_1 - c^2)}{c^2d_2}, a_2 = \frac{id_3}{c^2d_2}, a_3 = \frac{id_4}{\xi\ c^2d_2}, a_4 = \frac{ik_1}{cd_2}, a_5 = -\frac{id_3}{c^2d_1}, a_6 = \frac{(d_2 - c^2)}{d_1\ c^2},$$

$$a_7 = \frac{d_4}{\xi\ c^2d_1}, a_8 = \frac{k_1}{cd_1}, a_9 = \frac{id_5}{\xi\ c^2}, a_{10} = \frac{2d_5}{\xi^2c^2}, a_{11} = i \in k_0'\xi,$$

$$a_{12} = \frac{-1 + c^2k_0}{c^2}, a_{13} = -d_6, a_{16} = a_6 - \frac{1}{c^2},$$

$$a_{20} = \frac{a_{13}}{c^2} - a_{10}, a_{21} = a_1 - \frac{1}{c^2}, r_i = -\frac{\Delta_2}{\Delta_1}, l_i = \frac{\Delta_3}{\Delta_1}, t_i = -\frac{\Delta_4}{\Delta_1},$$

$$\Delta_1 = \frac{(-m_i^2 - 1 + c^2k_0)}{c^6}[(m_i^2 + a)(-m_i^2 + b) - \frac{d_4d_5}{\xi^2d_1}] - \frac{im_i^2 \in k_0'k_1\xi(-m_i^2 + b)}{d_1c^3},$$

$$\Delta_2 = \frac{(-m_i^2 - 1 + c^2k_0)}{c^6}[\frac{im_id_3}{d_1}(-m_i^2 + b) + \frac{im_id_4d_5}{\xi^2d_1}] + \frac{m_ik_0'k_1\xi(-m_i^2 + b)}{d_1c^3},$$

$$\Delta_3 = \frac{im_id_5(-m_i^2 - 1 + c^2k_0)}{\xi c^6}[\frac{id_3}{d_1} - (m_i^2 + a)] + \frac{m_id_5 \in k_0'k_1(m_i^2 + i)}{d_1c^3},$$

$$\Delta_4 = \frac{\in \xi\ k_0'(-m_i^2 + b)}{c^4}[\frac{d_3m_i^2}{d_1} + (m_i^2 + a)] + \frac{d_4d_5 \in k_0'(m_i^2 + i)}{d_1\xi\ c^4},$$

$$a = \frac{d_2 - c^2}{d_1}, b = (-1 + c^2d_6 - \frac{2d_5}{\xi^2}),$$

$$k_0 = \tau_0 + i\omega^{-1}, k_0' = \eta_0\tau_0 + i\omega^{-1}, k_1 = \tau_1 + i\omega^{-1}.$$

(i) Leaky Lamb waves

The most appropriate choice of total solutions for solid media having finite thickness (plate of thickness 2d) sandwiched between two liquid half spaces is given by equations (3) and

$$\phi_{L_1} = E_5e^{\gamma_L(z+d)}J_0(\xi r)e^{-i\omega t}, -\infty < z < -d, \tag{28}$$

$$\phi_{L_2} = F_6 e^{-\gamma_L (z-d)} J_0(\xi r) e^{-i\omega t}, d < z < \infty. \tag{29}$$

(ii) Nonleaky Lamb waves

The corresponding solutions for a solid plate of finite thickness 2d sandwiched between two finite liquid layers of thickness h is given by equations (3) and

$$\phi_{L_1} = E_5 Sinh\gamma_L \left[z + (d+h)\right] J_0(\xi r) e^{-i\omega t}, -(d+h) < z < -d, \tag{30}$$

$$\phi_{L_2} = F_6 Sinh\gamma_L \left[z - (d+h)\right] J_0(\xi r) e^{-i\omega t}, d < z < d+h. \tag{31}$$

The main difference between nonleaky Lamb waves and leaky Lamb waves is that the functions $\phi_{L_1}$and $\phi_{L_2}$are chosen in such a way that the acoustical pressure is zero at $z = \mp(d+h)$. In other words, ϕ_{L_1} and ϕ_{L_2}here are of standing wave solutions for nonleaky Lamb waves and for leaky Lamb waves they are of traveling waves.

Boundary Conditions

The boundary conditions at the solid – liquid interfaces $z = \pm d$ to be satisfied are as follows:

(i) The magnitude of the normal component of the stress tensor of the plate should be equal to the pressure of the liquid

$$(t_{zz})_L = (t_{zz})_S . \tag{32}$$

(ii) The tangential component of the stress tensor should be zero.

$$(t_{zr})_S = 0, \tag{33}$$

(iii) The tangential component of the couple stress tensor should be zero.

$$(m_{z\theta})_S = 0, \tag{34}$$

(iv) The normal velocity component of the solid should be equal to that of the liquid.

$$(\bar{u}_z)_S = (\bar{w}_L) \tag{35}$$

(v) The thermal boundary condition is given by

$$T_z + HT = 0. \tag{36}$$

where H is the surface heat transfer coefficient . Here H $\rightarrow$ 0 corresponds to thermally insulated boundaries and $H \rightarrow \infty$ refers to isothermal one.

4. Derivation of the dispersion equations

In this section we apply the already shown formal solutions to study the specific situations in which the fluid is inviscid.

(i) Leaky Lamb Waves

We consider an isotropic micropolar thermoelastic plate with cubic symmetry completely immersed in a inviscid liquid. The plate thickness is 2d and thus the lower and upper portions of the fluid extend from z = d to ∞ and z = -d to $-\infty$ respectively. The partial waves in this case are in both the plate and the fluid. The appropriate formal solutions for the plate and fluids are those given by equations (25), (28) and (29). By applying the boundary conditions (32) – (36) at $z = \pm d$and subsequently requiring nontrivial values of the partial wave amplitudes E_k and F_k, k = 1,2,3, 4; E_5 , F_6 and $\gamma_L \neq 0$, we arrive at the characteristic dispersion equations after lengthy but straightforward algebraic reductions and manipulations

$$AT1\ [T_1T_3]^{\pm 1} + \frac{\rho_L\omega^2 T_5}{\rho\gamma_L} AT21\,[T_1T_3]^{\pm 1} = AT2\ [T_1T_2]^{\pm 1} + \tag{37}$$

$$\text{AT3}\ [T_1T_4]^{\pm 1} + AT4\ [T_2T_3]^{\pm 1} + AT5\ [T_2T_4]^{\pm 1} + AT6\ [T_3T_4]^{\pm 1} \quad +$$

$$\frac{\rho_L\omega^2 T_5}{\rho\gamma_L}\Big\{AT22\ [T_1T_2]^{\pm 1} + AT23\ [T_1T_4]^{\pm 1} + AT24\ [T_2T_3]^{\pm 1} + \text{AT25}\ [T_2T_4]^{\pm 1} +$$

$$AT26\ [T_3T_4]^{\pm 1}\}$$

for stress free thermally insulated boundaries$(H \rightarrow 0)$ **of the plate**.

(ii) Nonleaky Lamb Waves

We consider an isotropic micropolar thermoelastic plate with cubic symmetry bordered with layers of inviscid liquid on both sides.

The appropriate formal solutions for the plate and fluids are those given by equations (25), (30) and (31). By applying the boundary conditions (32) – (36) at $z = \pm d$ and subsequently requiring nontrivial values of the partial wave amplitudes E_k and F_k, k = 1,2,3,4; E_5 ,F_6 and $\gamma_L \neq 0$, we arrive at the characteristic dispersion equations after lengthy but straightforward algebraic reductions and manipulations

$$AT1\ [T_1T_3]^{\pm 1} + \frac{\rho_L\omega^2}{\rho\gamma_L} AT21\,[T_1T_3]^{\pm 1} = \tag{38}$$

$$\text{AT2 } [T_1T_2]^{\pm1}+AT3\ [T_1T_4]^{\pm1}+AT4\ [T_2T_3]^{\pm1}+AT5\ [T_2T_4]^{\pm1}+AT6\ [T_3T_4]^{\pm1}\ +$$

$$\frac{\rho_L\omega^2}{\rho\gamma_L}\Big\{AT22\ [T_1T_2]^{\pm1}+AT23\ [T_1T_4]^{\pm1}+AT24\ [T_2T_3]^{\pm1}+\text{AT25}\ [T_2T_4]^{\pm1}+ AT26\ [T_3T_4]^{\pm1}\}$$

for stress free thermally insulated boundaries$(H\to 0)$ **of the plate**.

$$AT2=(g_{52}g_{61}-g_{51}g_{62})[(g_1-g_{13})g_{34}-(g_1-g_{14})g_{33}],$$

$$AT3=(g_{51}g_{64}-g_{54}g_{61})[(g_1-g_{13})g_{32}-(g_1-g_{12})g_{33}],$$

$$AT4=(g_{53}g_{62}-g_{52}g_{63})[(g_1-g_{11})g_{34}-(g_1-g_{14})g_{31}],$$

$$AT5=(g_{54}g_{62}-g_{52}g_{64})[(g_1-g_{13})g_{34}-(g_1-g_{14})g_{33}],$$

$$AT6=(g_{54}g_{63}-g_{53}g_{64})[(g_1-g_{11})g_{32}-(g_1-g_{12})g_{31}],$$

$$AT21=(g_{53}g_{61}-g_{51}g_{63})[g_{34}r_2-g_{32}r_4],\ AT22=(g_{52}g_{61}-g_{51}g_{62})[g_{34}r_3-g_{33}r_4],$$

$$AT23=(g_{51}g_{64}-g_{54}g_{61})[g_{32}r_3-g_{33}r_2],\ AT24=(g_{53}g_{62}-g_{52}g_{63})[g_{34}r_1-g_{31}r_4],$$

$$AT25=(g_{54}g_{62}-g_{52}g_{64})[g_{34}r_3-g_{33}r_1],\ AT26=(g_{54}g_{63}-g_{53}g_{64})[g_{32}r_1-g_{31}r_2].$$

$$T_i=Tan\ \xi m_i d, g_1=d_7 i\xi, g_{1i}=i\omega\ k_1t_i, g_{2i}=\xi\ m_ir_id_1,$$

$g_{3i}=i\xi\ r_id_8-l_id_4,\ g_{4i}=\xi\ m_id_2\ ,\ g_{5i}=\xi\ m_il_i,\ g_{6i}=\xi\ m_it_i,$ i = 1, 2, 3, 4; $T_5=\tan\ \xi\gamma_{\mathrm{L}}h.$

Here the exponent +1 refers to skew-symmetric and -1 refers to symmetric modes.

Equations (37) - (38) are the most general dispersion relations involving wave number and phase velocity of various modes of propagation in micropolar thermoelastic cubic crystal plate bordered with layers of inviscid liquid or half spaces on both sides.

5. Special cases

If we remove the liquid layers or half spaces on both sides, then we shall be left with the problem of wave propagation in micropolar thermoelastic cubic crystal plate. To do this, we shall put $\rho_L = 0$ in equations (37) – (38). The reduced secular equations for stress free thermally insulated boundaries($H \to 0$) for the said case are given by

AT1 $[T_1T_3]^{\pm 1} = AT2\ [T_1T_2]^{\pm 1} + AT3\ [T_1T_4]^{\pm 1} + AT4\ [T_2T_3]^{\pm 1} +$
$AT5\ [T_2T_4]^{\pm 1} + AT6\ [T_3T_4]^{\pm 1}$

5.1 Micropolar thermoelastic plate

In this case, $A_1 = \lambda + 2\mu + K$, $A_2 = \lambda$, $A_3 = \mu + K$, $A_4 = \mu$, $B_3 = \gamma$ The reduced secular equations agree with Kumar and Partap [19].

5.2 Micropolar elastic plate

In this case,$A_1 = \lambda+2\mu+K$,$A_2 = \lambda$, $A_3 = \mu+K$,$A_4 = \mu$,$B_3 = \gamma$, and thermal parameters $K^* = C^* = \nu = 0$
The reduced secular equations agree with Kumar and Partap [20].

6. Amplitudes of displacements, microrotation and temperature distribution

In this section the amplitudes of displacement components, microrotation and temperature distribution for symmetric and skew-symmetric modes of plate waves can be obtained as

$$(u_r)_{sym}, (u_r)_{asym} = \sum_{i=1}^{4} (E_i Cos\ \xi m_i z, \qquad F_i Sin\ \xi m_i z) J_1(\xi r) e^{-i\omega t},$$

$$(u_z)_{sym}, (u_z)_{asym} = \sum_{i=1}^{4} r_i (F_i Sin \xi m_i z, \qquad E_i Cos \xi m_i z) J_0(\xi r) e^{-i\omega t},$$

$$(\phi_\theta)_{sym}, (\phi_\theta)_{asym} = \sum_{i=1}^{4} l_i (F_i Sin \xi m_i z, \qquad E_i Cos \xi m_i z) J_1(\xi r) e^{-i\omega t},$$

$$(T)_{sym}, (T)_{asym} = \sum_{i=1}^{4} t_i (E_i Cos \xi m_i z, \qquad F_i Sin \xi m_i z) J_0(\xi r) e^{-i\omega t}.$$

7. Example results

For numerical computations, we take the following values of relevant parameters for micropolar medium with cubic symmetry as

$$\mathrm{A}_1 = 19.6 \times 10^{10} N/m^2, A_2 = 11.7 \times 10^{10} N/m^2, A_3 = 5.6 \times 10^{10} N/m^2,$$
$$\mathrm{A}_4 = 4.3 \times 10^{10} N/m^2, B_3 = 0.98 \times 10^{-9} N$$

Micropolar parameters are

$$\rho = 1.74 \times 10^3 Kg/m^3, \lambda = 9.4 \times 10^{10} N/m^2, \mu = 4.0 \times 10^{10} N/m^2,$$

$$K = 1.0 \times 10^{10} N/m^2, \gamma = 0.779 \times 10^{-9} N, j = 0.2 \times 10^{-19} m^2.$$

Thermal parameters are

$$\tau_0 = 6.131 \times 10^{-13} \sec, \tau_1 = 8.765 \times 10^{-13} \sec, \in = 0.028, T_0 = 298^0 K,$$
$$\mathrm{C}^* = 1.04 \times 10^3 J/Kg \deg,$$

$$K^* = 1.7 \times 10^6 J/m \sec \deg, \nu = 2.68 \times 10^6 N/m^2 \deg,$$

The liquid taken for the purpose of numerical calculations is water and the speed of sound in water given by $c_L = 1.5 \times 10^3 m/\sec$.
In general, wave number and phase velocity of the waves are complex quantities, therefore, the waves are attenuated in space. If we write

$$c^{-1} = v^{-1} + i\omega^{-1} q \tag{39}$$

then $\xi = K_1 + iq$, where $K_1 = \omega/v$ and q are real numbers. This shows that v is the propagation speed and q is attenuation coefficient of waves. Upon using equation (39) in secular equations (37) and (38), the value of propagation speed v and attenuation coefficient q for different modes of wave propagation can be obtained.
The dotted curves refer to L-S theory and solid curves correspond to G-L theory of thermoelasticity.
The phase velocity of symmetric and skew-symmetric modes of wave propagation in the context of L-S and G-L theories of thermoelasticity have been computed for various values of wave number from dispersion equations (37) and (38) for stress free thermally insulated micropolar thermoelastic cubic crystal plate and have been represented graphically for different modes (n = 0 to n =

2) in figures 1 and 2 for leaky Lamb waves and in figures 5 and 6 for nonleaky Lamb waves.

The variation of attenuation coefficient with wave number for lowest symmetric and skew-symmetric modes (n = 0) of wave propagation in the context of L-S and G-L theories of thermoelasticity for stress free thermally insulated micropolar thermoelastic cubic crystal plate is represented graphically in figures 3 and 4 for leaky Lamb waves and in figures 7 and 8 for nonleaky Lamb waves. Figures 9 - 16 depict the variations of symmetric and skew-symmetric amplitudes of displacements u_r, u_z, microrotation ϕ_θ and temperature distribution T in the context of L-S and G-L theories of thermoelasticity for stress free thermally insulated boundary.

The phase velocities of higher modes of propagation, symmetric and skew-symmetric for leaky and nonleaky Lamb waves as evident from figures 1, 2, 5 and 6 attain quite large values at vanishing wave number which sharply slashes down to become steady and asymptotic with increasing wave number.

Phase velocity

The phase velocities of lowest symmetric leaky and nonleaky Lamb wave modes of propagation become dispersionless i.e. remain constant with variation in wave number. It is evident from figure 1 and figure 5 that (a) phase velocity profiles for L-S and G-L theory coincide for symmetric modes (n = 0 and n = 2) of propagation (b) for n = 1, phase velocity for L-S theory is less than in case of G-L theory for wave number $\xi \leq 2.2$; phase velocity for L-S theory is slightly more than in case of G-L theory for wave number lying between 2.2 and 3.2; phase velocity profiles for L-S and G-L theory coincide for wave number $\xi \geq 3.2$.

For skew-symmetric leaky Lamb wave modes of propagation, we notice the following from figure 2: (a) for n = 0, phase velocity for L-S theory is less than in case of G-L theory for wave number $\xi \leq 1.2$; phase velocity for L-S theory is more than in case of G-L theory for wave number lying between 1.2 and 2.2; phase velocity profiles for L-S theory and G-L theory coincide for wave number $\xi \geq 2.2$ (b) for n = 1, phase velocity for L-S theory is slightly more than in case of G-L theory for wave number $\xi \leq 1.2$; phase velocity profiles for L-S theory and G-L theory coincide for wave number lying between 1.2 and 2.4; phase velocity for L-S theory is less than in case of G-L theory for wave number $\xi \geq 2.4$ and $\xi \leq 4.6$; phase velocity profiles for L-S theory and G-L theory coincide for wave number $\xi \geq 4.6$(c) phase velocity for L-S theory is slightly more than in case of G-L theory for wave number $\xi \leq 1.2$ and for wave number lying between 2.8 and 4.2; phase velocity for L-S theory is less than in case of G-L theory for wave number lying between 1.2 and 2.8; phase velocity profiles for L-S theory and G-L theory coincide for wave number $\xi \geq 4.2$.

For skew-symmetric nonleaky Lamb wave modes of propagation, we notice the following from figure 6: (a) for lowest mode (n = 0) phase velocity for L-S theory is more than in case of G-L for wave number $\xi \leq 1.2$; phase velocity for L-S theory is less than in case of G-L theory for wave number $\xi \geq 1.2$ and $\xi \leq 2.2$; phase velocity profiles coincide for wave number $\xi \geq 2.2$ (b) phase velocity profiles for L-S theory and G-L theory coincide for modes n = 1 and n = 2.

Attenuation coefficients

For symmetric leaky and nonleaky Lamb wave mode (n = 0), the magnitude of attenuation coefficient for L-S and G-L theories increases upto 123.9 and 113.4 respectively in the region $0.2 \leq \xi \leq 5.2$ at $\xi = 5.2$ It is evident from figure 3 and figure 7 that symmetric modes of propagation have same attenuation coefficient for wave number $\xi \leq 2.2$ and have higher attenuation coefficient in L-S theory followed by G-L theory for wave number $\xi \geq 2.2$ and $\xi \leq 5.2$.
The attenuation coefficient for lowest skew-symmetric leaky and nonleaky Lamb wave mode (n = 0) has negligible variation with wave number in G-L theory of thermoelasticity as evident from figure 4 and figure 8. For lowest skew-symmetric leaky Lamb wave mode, the attenuation coefficient has negligible variation with wave number in L-S theory of thermoelasticity in the region $0.2 \leq \xi \leq 3.2$ and attains high values 1577 and 1655 at $\xi = 4.2$ and at $\xi = 5.2$ respectively in the $3.2 \leq \xi \leq 5.2$ as evident from figure 4. For lowest skew-symmetric nonleaky Lamb wave mode, attenuation coefficient for L-S theory attains maximum value 997.5 in the region $0.2 \leq \xi \leq 3.2$ at $\xi = 1.2$ and decreases sharply to nearly zero with the increase in wave number as noticed from figure 8.

Amplitudes

The displacement u_r and temperature distribution T of the plate is minimum at the centre and maximum at the surfaces for symmetric mode and zero at the centre and maximum at the surfaces for skew-symmetric mode as evident from figures 9, 10, 15 and 16 respectively. From figure 11 and figure 12, it is noticed that the values of the displacement u_z of the plate is zero at the centre and maximum at the surfaces for symmetric mode and maximum at the centre and minimum at the surfaces for skew-symmetric mode. It is evident from figure 13 and figure 14 that the value of microrotationϕ_θ of the plate is zero at the centre, minimum at the bottom surface and maximum at the top surface of the plate for symmetric mode and minimum at the centre and maximum at the surfaces for skew-symmetric mode. $(u_r)_{sym}$,$(u_r)_{asym}$,$(u_z)_{sym}$,$(u_z)_{asym}$,$(\phi_\theta)_{sym}$, $(\phi_\theta)_{asym}$,$(T)_{sym}$and$(T)_{asym}$ correspond to the values of u_r,u_z,ϕ_θ and

T for symmetric and skew -symmetric modes respectively.
The values of the symmetric displacements u_r of the plate in case of G-L theory are slightly higher in comparison to L-S theory. The values of the skew-symmetric displacements u_r and symmetric displacements u_z of the plate are nearly same in case of L-S and G-L theories. The values of the skew-symmetric displacements u_z of the plate in case of G-L theory are more in comparison to L-S theory. The values of the microrotation ϕ_θ of the plate are exactly same in case of L-S and G-L theories for symmetric and skew-symmetric modes. The values of the temperature distribution T of the plate in case of G-L theory are less in comparison to L-S theory for symmetric and skew-symmetric modes.

8. Conclusions

(i) The propagation of leaky and nonleaky Lamb waves in a homogenous isotropic micropolar thermoelastic cubic crystal plate bordered with layers or half spaces of inviscid liquid subjected to stress free boundary conditions has been studied in context of Lord and Shulman (L-S) and Green and Lindsay (G-L) theories of thermoelasticity (ii) The secular equations for symmetric and skew-symmetric leaky and nonleaky Lamb wave modes of propagation are derived (iii) The phase velocities of lowest symmetric leaky and nonleaky Lamb modes of propagation become dispersionless i.e. remain constant with variation in wave number. The phase velocities of higher leaky and nonleaky Lamb modes of propagation, symmetric and skew-symmetric attain quite large values at vanishing wave number which sharply slashes down to become steady and asymptotic with increasing wave number (iv) The variation of phase velocity and attenuation coefficient with wave number for symmetric modes (n = 0) of wave propagation in the context of L-S and G-L theories of thermoelasticity for stress free thermally insulated micropolar thermoelastic cubic crystals is same for leaky Lamb waves and nonleaky Lamb waves (v) It is observed that behavior and trend of variations $(u_r)_{asym}$and $(T)_{asym}$ is similar to $(u_z)_{sym}$ and that of $(u_r)_{sym}$ resembles with $(T)_{sym}$. However the behavior and trend of variations $(u_z)_{asym}$ is opposite to that of $(u_r)_{sym}$and$(T)_{sym}$.

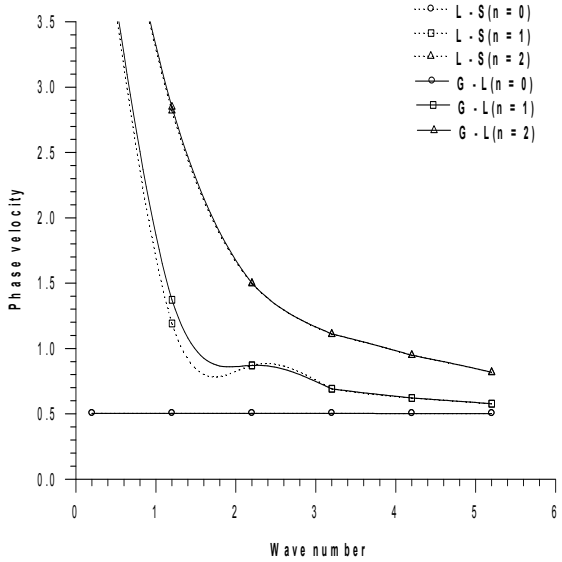

Fig.1 Variation of phase velocity of symmetric leaky Lamb wave modes

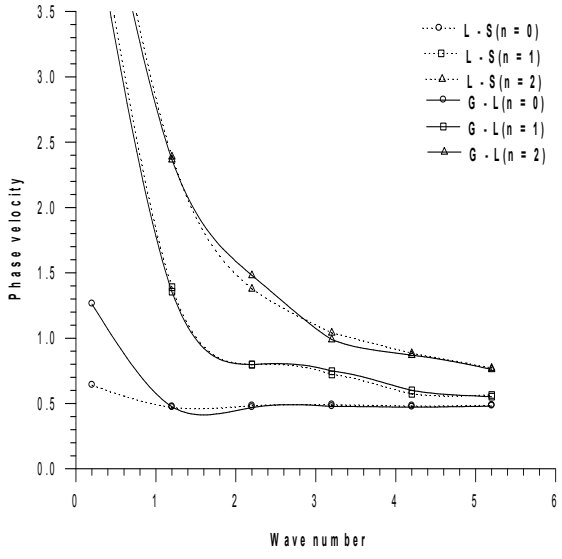

Fig.2 Variation of phase velocity of skew-symmetric leaky Lamb wave modes

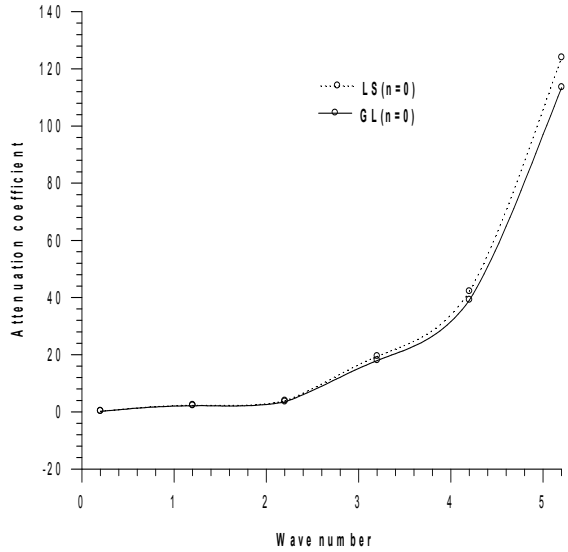

Fig.3 Variation of attenuation coefficient of symmetric leaky Lamb wave modes

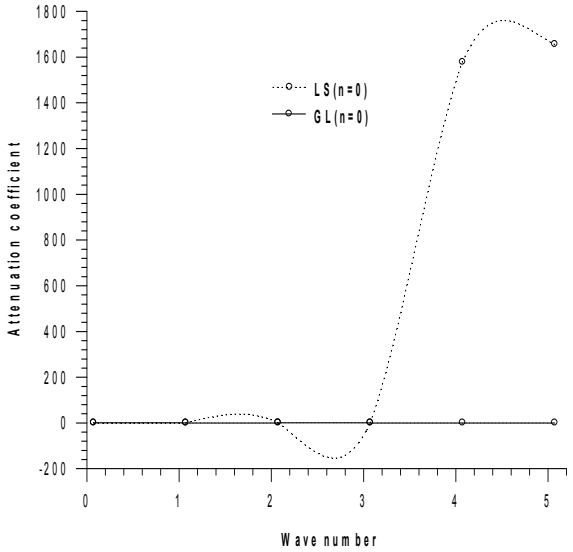

Fig.4 Variation of attenuation coefficient of skew-symmetric leaky Lamb wave modes

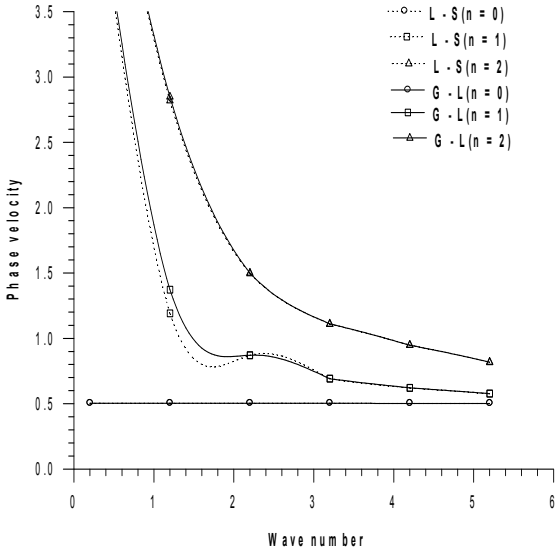

Fig.5 Variation of phase velocity of symmetric nonleaky Lamb wave modes

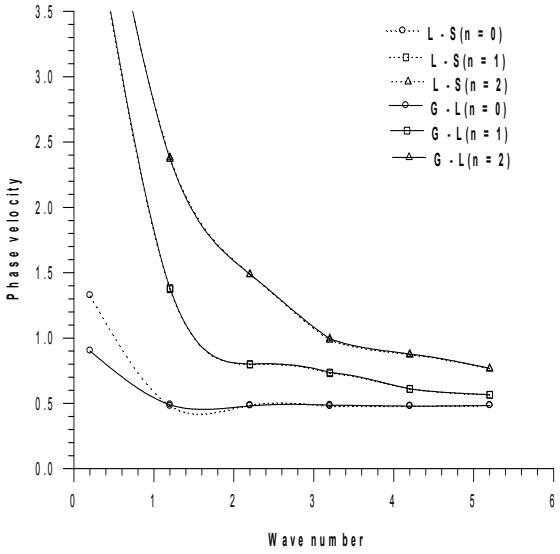

Fig.6 Variation of phase velocity of skew-symmetric nonleaky Lamb wave modes

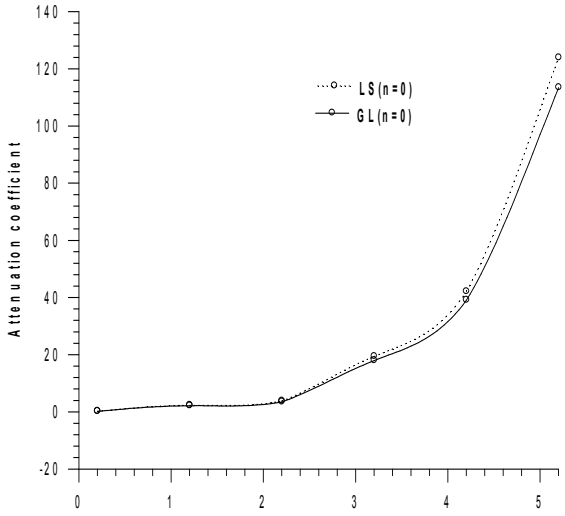

Fig.7 Variation of attenuation coefficient of symmetric nonleaky Lamb wave modes

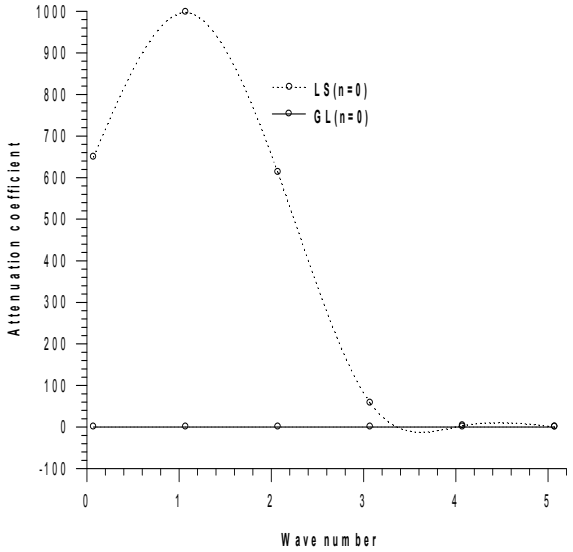

Fig.8 Variation of attenuation coefficient of skew-symmetric nonleaky Lamb wave modes

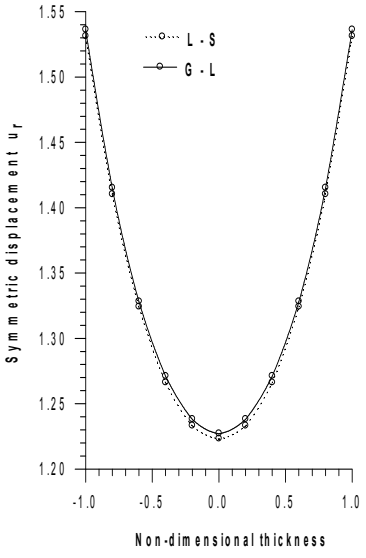

Fig. 9 Amplitude of symmetric displacement u_r

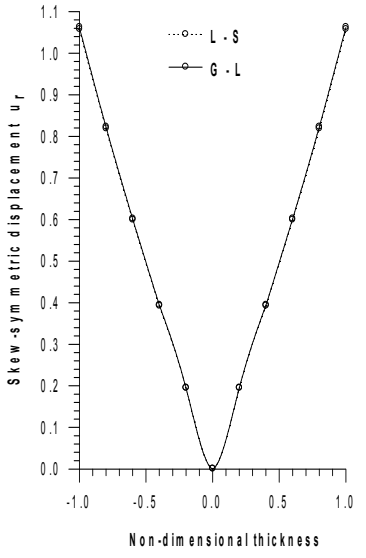

Fig.10 Amplitude of skew-symmetric displacement u_r

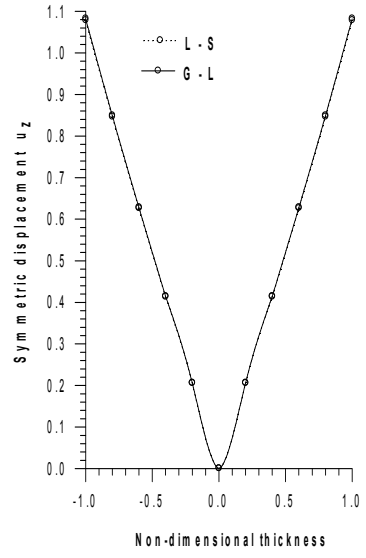

Fig.11 Amplitude of symmetric displacement u_z

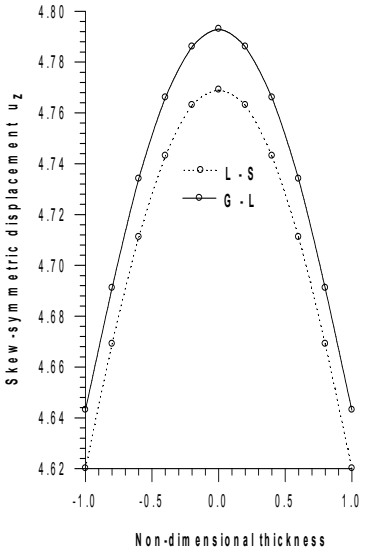

Fig.12 Amplitude of skew-symmetric displacement u_z

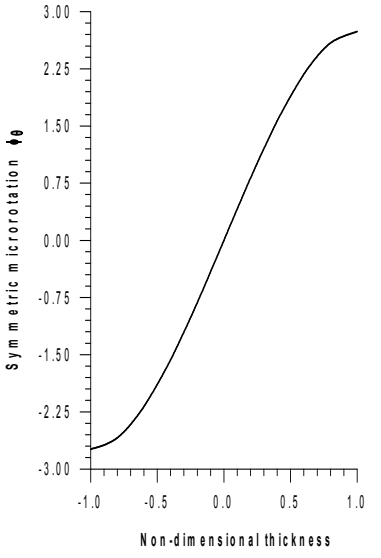

Fig.13 Amplitude of symmetric microrotation ϕ_θ

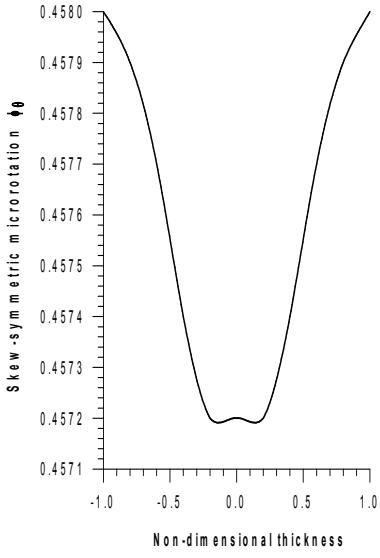

Fig.14 Amplitude of skew-symmetric microrotation ϕ_θ

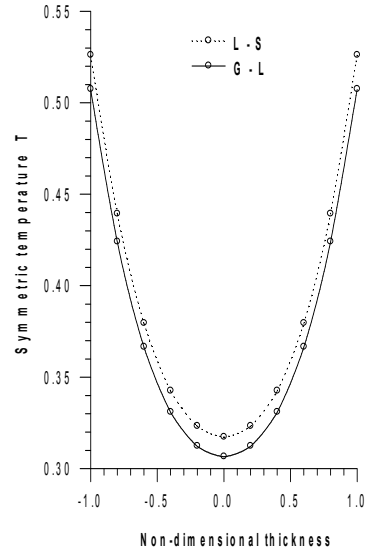

Fig.15 Amplitude of symmetric temperature T

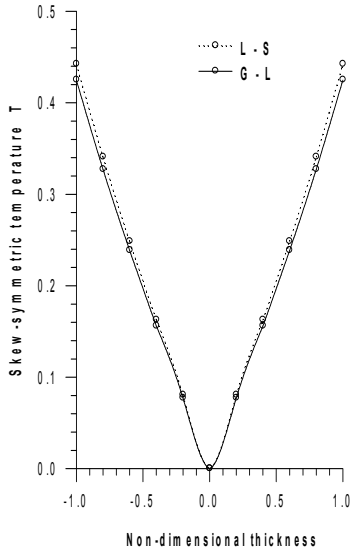

Fig.16 Amplitude of skew-symmetric temperature T

References

[1] H. Lamb, *On waves in an elastic plate*, Phil. Trans.Roy. Soc., London, Ser. A, **93** (1917), 114-128.

[2] J.Wu, Z. Zhu, The propagation of Lamb waves in a plate bordered with layers of liquid, *J. Acoust. Soc. Am.*, **91** (1992), 861-867.

[3] Z. Zhu, J.Wu, The propagation of Lamb waves in a plate bordered with a viscous fluid, *J. Acoust. Soc. Am.*, **98** (1995), 1057-1064.

[4] A.H. Nayfeh, P.B. Nagy, Excess attenuation of Leaky Lamb waves due to viscous fluid loading. *J. Acoust. Soc. Am.*, **101** (1997), 2649-2658.

[5] A.C. Eringen, Linear theory of micropolar elasticity, *J. of Mathematics and Mechanics*, **15** (1966), 909-923.

[6] A.C. Eringen, *Foundations of micropolar thermoelasticity*, Int. Cent. For Mech. Studies, Course and Lectures, No. 23, Springer – Verlag, Wien, 1970.

[7] M. Nowacki, *Couple-stresses in the theory of thermoelasticity*, In: Parkus H, Sedov LI(eds.) Proceeding of IUTAM Symposia, Vienna, 1966.

[8] D.H. Chung, W.R. Buessem, The elastic anisotropy of crystals, *J. Appl. Phys.*, **38** (1967), 2010-2012.

[9] K.-HC Lie, J.S. Koehler, The elastic stress field produced by a point force in a cubic crystal, *Adv. Phys.*, **17** (1968), 421-478.

[10] S. Minagawa, K. Arakawa, M.Yamada, Dispersion curves for waves in a cubic micropolar medium with reference to estimations of the material constants for diamond, *Bull. JSME*, **24** (1981), 22-28.

[11] R. Kumar , L. Rani, Elastodynamics of time harmonic sources in a thermally conducting cubic crystal, *International Journal of Applied Mechanics and Engineering*, **8** (2003), 637-650.

[12] R. Kumar, P. Ailawalia, Elastodynamics of inclined loads in a micropolar cubic crystals, *Mechanics and Mechanical Engineering*, **9** (2005), 57-75.

[13] R. Kumar, P. Ailawalia, Time harmonic sources at micropolar thermoelastic medium possessing cubic crystals with one relaxation time, *European Journal of Mechanics A/Solids*, **25** (2006), 271-282.

[14] R. Kumar, M. Singh, Thermoelastic plane waves at imperfectly bounded interface of generalized thermoelastic cubic crystal solids, Mechanics of Advanced Materials and Structures, **14** (2007), 427-437.

[15] R. Kumar, T. Kansal, Analysis of wave motion in transversely isotropic generalized thermoelastic diffusive plate, *Journal of Technical Physics*, **50** (2009), 3-26.

[16] J.N. Sharma, S. Kumar, Lamb waves in micropolar thermoelastic solid plates immersed in liquid with varying temperature, *Meccanica*, **44** (2009), 305-319.

[17] H.W. Lord, Y. Shulman, A generalized dynamical theory of thermoelasticity, *J. Mech. Phys. Solids*, **15** (1967), 299-309.

[18] A.E. Green, K.A. Lindsay, Thermoelasticity, *J. Elasticity*, **2** (1972), 1-7.

[19] R.Kumar, G.Partap, Wave propagation in a circular crested micropolar generalized thermoelastic plate, *Buletinul Institutului Politehnic din Iasi*, **3** no. 4 (2007), 53-72.

[20] R.Kumar, G.Partap, Rayleigh Lamb waves in micropolar isotropic elastic plate, *Applied Mathematics and Mechanics*, **27** (2006), 1049-1059.